A typology of photoreceptor gene expression patterns in the mouse

Joseph C. Corbo*, Connie A. Myers*, Karen A. Lawrence*, Ashutosh P. Jadhav†, and Constance L. Cepko†‡

*Department of Pathology and Immunology, Washington University School of Medicine, St. Louis, MO 63110; and †Department of Genetics and Howard Hughes Medical Institute, Harvard Medical School, Boston, MA 02115

Contributed by Constance L. Cepko, June 12, 2007 (sent for review January 24, 2007)

Mutations in photoreceptor-enriched genes have been implicated in dozens of human retinal diseases, yet no systematic analysis of rod and cone gene expression patterns has been carried out. In addition, although cone photoreceptor loss accounts for much of the morbidity of retinal disease, relatively few cone-specific genes are known. In this study, we carried out microarray and *in situ* hybridization analyses of the mouse *Neural retina leucine zipper gene* (*Nrl*) mutant, which shows an *en masse* conversion of rods into cones, to establish a typology of photoreceptor gene expression and to identify novel cone-specific genes. We found a total of 18 new cone-enriched genes, some of which map near uncloned retinal disease loci. Several of these genes have a dorsal–ventral (D–V) pattern of expression similar to that of short- or medium-wavelength opsins. We carried out microarray analysis of dorsal and ventral microdissected WT retina and found additional photoreceptor genes with an asymmetric distribution. Overall, we found that photoreceptor genes fall on an expression spectrum from rod-specific to cone-specific, with many showing varying degrees of rod and cone coexpression. These expression patterns can be reliably predicted from microarray data alone. Our results demonstrate definitive molecular differences between rods and cones that may underlie the physiological differences between these two classes of photoreceptors.

blindness | cone photoreceptor | retina | rod photoreceptor

More than 180 genetic loci for human retinal disease have been mapped, and >120 causative genes have been identified (www.sph.uth.tmc.edu/RetNet/). Many of these genes are specifically expressed or highly enriched in photoreceptors (1), thus implicating this cell type in the majority of blinding diseases. Although in some forms of genetic blindness, such as retinitis pigmentosa, rods are preferentially affected early in the disease process, with time, cones are also involved (2). It is the loss of the latter cell type that eventually causes the most severe disability. The basis of the differential susceptibility of rods and cones to different genetic insults is not known in most cases, but there are clear indications that it correlates, in the early stages, with the expression pattern of the disease gene (i.e., whether it is expressed in rods, cones, or both). For this reason, it is of great importance to elucidate the precise expression patterns of retinal disease genes within rods and cones.

Despite the many well characterized physiologic differences between rods and cones (3), our knowledge of the underlying molecular determinants of these differences is rudimentary. This ignorance is attributable, in part, to the fact that nearly all well studied mammalian species have rod-dominant retinas with only a small percentage of cones (4). The scarcity of cones in these species has hampered biochemical and molecular studies of this clinically crucial cell type.

The *Nrl* mutant retina may represent a solution to the cone scarcity problem. Nrl is a transcription factor which is specifically expressed in rods (5). Molecular, ultrastructural, and electrophysiologic evidence suggests that in the *Nrl* mutant rod precursors differentiate as cones instead of rods (6). The net result is an all-cone retina. Although the $Nrl^{-/-}$ retina displays morphologic distortion of the outer nuclear layer (ONL) (likely secondary to the presence of an abnormally large number of cones) and the majority of the cones in this mutant express S-opsin and not M-opsin, we believe it represents a useful tool for the discovery of cone genes. Recent studies have begun to characterize the alterations in the transcriptome of the $Nrl^{-/-}$ retina (7). Here, we extend these studies by carrying out microarray and *in situ* hybridization (ISH) analysis of WT and $Nrl^{-/-}$ retinas and by comparing them wtih similar analyses of the *Nrl* target gene, photoreceptor-specific nuclear receptor (*Nr2e3*), done in ref. 8. We have used these data to identify novel cone-enriched disease gene candidates and to define a typology of photoreceptor gene expression in the mouse.

Results

Photoreceptor Genes Fall on a Continuous Spectrum from Cone-Specific to Rod-Specific. To evaluate the complements of rod and cone-specific transcripts in the mouse retina, we carried out an oligonucleotide-based microarray analysis of *Nrl* mutant and WT (C57BL/6) control retinas at the end of photoreceptor differentiation (P21) [supporting information (SI) Table 2]. We analyzed three biological replicates each of WT and $Nrl^{-/-}$ retinas, subjected them to pairwise comparisons, and identified up- and down-regulated genes by Wilcoxon's signed rank test. We found that there were 1,934 up-regulated and 991 down-regulated genes which were significantly changed in all three pairwise comparisons ($P = 0.002$). To obtain a smaller set of genes for more detailed characterization, we applied even more stringent criteria (see *Materials and Methods*) to these sets of up- and down-regulated genes to identify sets of 297 and 141 genes, respectively (SI Tables 3 and 4).

Next, we performed ISH on a subset of the dysregulated genes to validate the microarray (8, 38, and this study) results. We selected genes which were found to be up- or down-regulated in $Nrl^{-/-}$, $Nr2e3^{-/-}$, or $Crx^{-/-}$ by microarray. In addition, we also carried out ISH on a set of known photoreceptor genes that did not show transcriptional changes by microarray as controls. We characterized a total of 73 genes with photoreceptor expression and classified them into five categories based on their degree of rod- or cone-specificity without reference to the microarray data (Fig. 1, SI Figs. 4–8, and SI Table 5). Under the assumption that the *Nrl* mutation results in a complete transformation of rods into cones, genes with no residual expression in $Nrl^{-/-}$ were

Author contributions: J.C.C. and C.L.C. designed research; J.C.C., C.A.M., K.A.L., A.P.J., and C.L.C. performed research; J.C.C., C.A.M., K.A.L., and A.P.J. contributed new reagents/analytic tools; J.C.C., C.A.M., and K.A.L. analyzed data; and J.C.C. and C.L.C. wrote the paper.

The authors declare no conflict of interest.

Freely available online through the PNAS open access option.

Abbreviations: ISH, *in situ* hybridization; D–V, dorsal–ventral; ONL, outer nuclear layer.

‡To whom correspondence should be addressed. E-mail: cepko@genetics.med.harvard.edu.

This article contains supporting information online at www.pnas.org/cgi/content/full/0705465104/DC1.

classified as rod-specific. Those genes whose expression was unchanged in the *Nrl* mutant were considered to be expressed at similar levels in rods and cones. Finally, those genes which in the WT retina had a cone-specific pattern of expression and which were markedly derepressed throughout the ONL in $Nrl^{-/-}$ were considered cone-specific. A number of coexpressed genes fell into two intermediate categories: rod > cone and cone > rod.

Photoreceptor Gene Expression Patterns Can Be Predicted from Microarray Data. To determine the extent to which the expression pattern of candidate photoreceptor genes can be predicted from microarray data alone, we ranked the 73 genes within these five expression categories according to the ratio of their average WT to $Nrl^{-/-}$ scores (WT:*Nrl* ratio) (SI Table 5). We found that the average WT:*Nrl* ratio for each of the five categories starting with rod-specific genes was as follows: 207.55, 6.56, 1.33, 0.69, and 0.23. A graph of the individual WT:*Nrl* ratios within each of these five categories indicates that there is a continuous distribution of values across all categories with some overlap between adjacent categories (Fig. 1*F*). Despite this overlap, it is possible to choose WT:*Nrl* ratio cut-off thresholds between the five categories (3, 2, 1, and 0.5) which permit correct classification of 75% of the 73 genes from microarray data alone. The 25% of genes that were incorrectly classified always fell into a class immediately adjacent to the predicted one. These minor discrepancies could relate to the fact that ISH is not a quantitative methodology and that, in some cases, the transcriptional isoform detected by the ISH probe may differ from that detected by the microarray probe set. Overall, analysis of the WT:*Nrl* ratio permits very accurate prediction of photoreceptor expression patterns.

To further evaluate the possibility of predicting photoreceptor gene expression patterns from microarray data, we carried out a comparison of our present data set with one generated for $Nr2e3^{-/-}$ retinas at P21 (8). In the study reported in ref. 8, we found two different patterns of cone gene derepression in $Nr2e3^{-/-}$. Genes showing "Type I" depression showed uniform expression throughout the entire $Nr2e3^{-/-}$ ONL, a pattern very similar to what is seen in $Nrl^{-/-}$. In contrast, genes with "Type II" derepression displayed a punctate pattern of expression in scattered cells throughout the $Nr2e3^{-/-}$ ONL. These same Type II genes show uniform derepression throughout the ONL in $Nrl^{-/-}$. We concluded from these facts that, in the case of Type I genes, *Nr2e3* mediates almost all of the repressive activity of *Nrl*. However, in the case of Type II genes, *Nr2e3* appears to be responsible for only a portion of the repression activity of *Nrl*.

Given these facts, we hypothesize that genes showing Type I derepression in $Nr2e3^{-/-}$ should demonstrate an increase in their microarray score (relative to WT) of similar magnitude to that seen in $Nrl^{-/-}$. In contrast, we predict that Type II cone genes will show an increase of considerably lower magnitude in $Nr2e3^{-/-}$ than in $Nrl^{-/-}$. To test this hypothesis, we performed ISH for 37 cone-enriched genes on the $Nr2e3^{-/-}$ retina (8, 38) Of these, 24 probes gave a sufficiently strong signal to classify the *Nr2e3* derepression pattern as Type I or II (Table 1 and SI Table 6). Remarkably, when these 24 genes are ranked according to the ratio of their $Nrl^{-/-}$ and $Nr2e3^{-/-}$ microarray scores (*Nrl*:*Nr2e3* ratio), the ratios were perfectly predictive of the pattern of expression. All cone genes with Type I derepression have an *Nrl*:*Nr2e3* ratio less than two, and all those with Type II derepression have a ratio greater than two (SI Table 7).

To determine the percentage of all cone genes that are likely to have Type I or II derepression in $Nr2e3^{-/-}$, we ranked all 297 genes which showed up-regulation in $Nrl^{-/-}$ (under stringent criteria) by their *Nrl*:*Nr2e3* ratio. Under the assumption that all rods are transfated into cones in $Nrl^{-/-}$, this list is likely to include many, if not most, highly cone-enriched genes which are expressed at moderate to high levels in the mouse. Surprisingly, we found that only 16% of the genes in this list had *Nrl*:*Nr2e3* ratios less than two (SI Table 7). This result implies that *Nr2e3* may account for the full repression activity of *Nrl* on only a small fraction of all cone genes. The remaining 84% of cone genes which are predicted to show Type II depression in $Nr2e3^{-/-}$ must therefore be repressed in rods directly by Nrl itself, or by another, currently unidentified downstream repressor (or repressors) as suggested in ref. 8.

An additional study of a cone-enriched retina, generated by loss

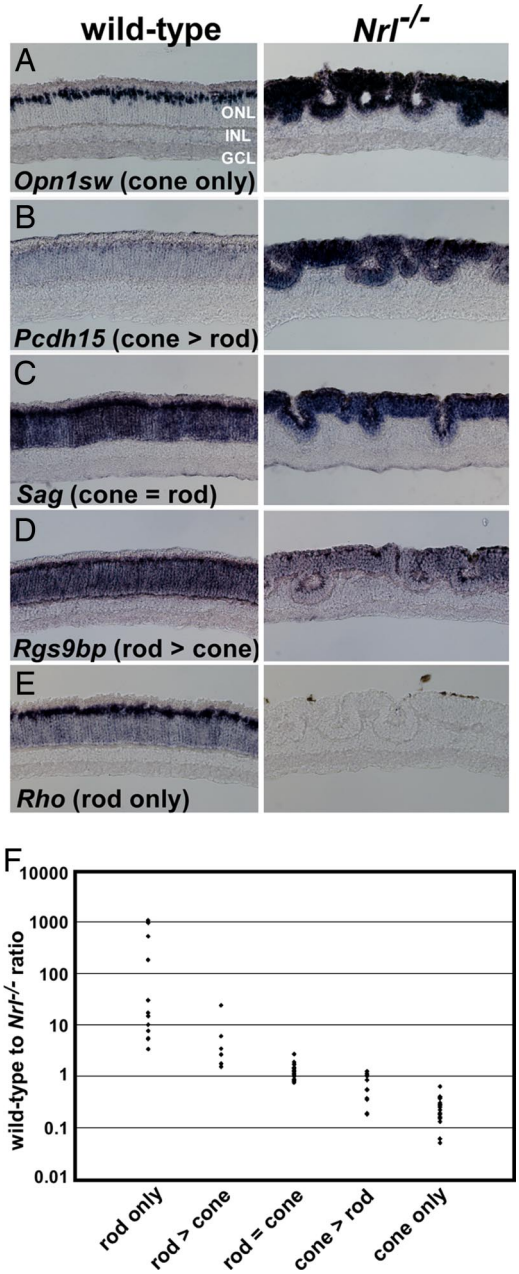

Fig. 1. Photoreceptor gene expression patterns fall on a spectrum from cone-specific to rod-specific. (*A–E*) Typical examples of each of the five photoreceptor gene expression categories: cone only (i.e., no rod expression), cone > rod (expressed in both photoreceptor cell types, but at higher levels in cones than rods), cone = rod (comparable levels of expression in rods and cones), rod > cone (expressed in both photoreceptor cell types, but at higher levels in rods than cones), and rod only (no cone expression). (*F*) Scatter plot showing the distribution of ratios of the WT (C57BL/6) microarray score to the $Nrl^{-/-}$ score for the 73 genes on which ISH was performed. The ratios are an average of three microarray scores from three separate experiments (see SI Table 5 for more details). INL, inner nuclear layer; GCL, ganglion cell layer.

Table 1. Summary of novel cone genes

Gene name	Expression pattern
RIKEN cDNA 4921511K06 gene (*4921511K06Rik*)	Cone (II) (V > D) + BP (subset)
Adrenergic receptor, beta 1 (*Adrb1*)	Cone (I) + BP
Gulonolactone (L-) oxidase (*Gulo*)	Cone (I)
Caspase 7 (*Casp7*)	Cone (II) + INL (subset)
Clathrin, light polypeptide (*Lcb*) (*Cltb*)	Cone (II) + INL/GCL
Adenosine monophosphate deaminase 2 (isoform L) (*Ampd2*)	Cone (II) + BP
Olfactomedin 1 (*Olfm1*)	Cone + INL/GCL
Hypothetical protein E130012K09 (*E130012K09*)	Cone (II) + BP
Diacylglycerol kinase, delta (*Dgkd*)	Cone (II)
Calcium binding protein 5 (*Cabp5*)	Cone (II) + BP
Hypothetical protein 7530404M11 (*7530404M11Rik*)	Cone (II) + BP (subset)
Histone 3, H2ba (*Hist3 h2ba*)	Cone > rod + INL/GCL
Reticulon 4 (*Rtn4*)	Cone > rod + INL/GCL
CAAX box 1 homolog C (human) (*Cxx1c*)	Cone (II?) + amacrine pattern
O-sialoglycoprotein endopeptidase (*Osgep*)	Cone (II?)
Ectonucleotide pyrophosphatase/phosphodiesterase 5 (*Enpp5*)	Cone > rod + INL/GCL
Chloride channel calcium activated 3 (*Clca3*)	Cone (I)
RIKEN cDNA A930018M24 gene (*A930018M24Rik*)	Cone + amacrine pattern

This table summarizes novel cone genes up-regulated in $Nrl^{-/-}$ and confirmed by ISH. ''Expression pattern'' includes a description of the retinal expression pattern of the gene in question. ''Cone > rod'' indicates pan-photoreceptor expression, but at higher levels in cones than in rods. BP, bipolar cells; RPE, retinal pigmented epithelium; INL, inner nuclear layer; GCL, ganglion cell layer. ''Amacrine pattern'' indicates expression at the vitread side of the inner nuclear layer and in the ganglion cell layer suggestive of expression in orthotopic and displaced amacrine cells, respectively (and possibly ganglion cells). (V > D) indicates a ventral greater than dorsal pattern of expression similar to S-opsin. (I), type I derepression in $Nr2e3^{-/-}$; (II), type II derepression in $Nr2e3^{-/-}$. Type I and type II derepression patterns are as described in ref. 8. A question mark indicates that the probe in question gave a weak signal but that the gene in question can be tentatively assigned the pattern indicated. For those probes that gave signals that were too weak to classify according to cone pattern or pattern of derepression in $Nr2e3^{-/-}$, no such annotation is included. Further details about the Genbank accession numbers of the probes used for ISH as well as about the identity of the putative human orthologs of the mouse genes in this table can be found in SI Tables 5 and 6, respectively.

of *Notch1* expression (9), showed similar up-regulation of a number of the cone-enriched genes identified in the $Nrl^{-/-}$ and $Nr2e3^{-/-}$ retinas. A limited cDNA microarray analysis of the *Notch1* mutant retina (data not shown) showed that of the 76 most up-regulated genes, 11 (14.5%) were cone-enriched as defined by stringent up-regulation in the $Nrl^{-/-}$ retina (SI Table 3).

Expression Patterns of Known and Novel Cone Genes. Given the importance of cone photoreceptors in human retinal disease, we decided to carry out a small-scale ISH screen of transcripts up-regulated in the $Nrl^{-/-}$ retina to identify novel cone genes. Only a small number of mouse cone genes are known (SI Table 6). Our study in ref. 8 of the $Nr2e3^{-/-}$ retina identified 10 cone-enriched genes, and the present screen identified an additional 18 cone-enriched genes (Table 1 and SI Table 6). Within photoreceptors, cone genes show either cone-specific or cone > rod expression patterns (Fig. 2 and SI Figs. 7 and 8). In addition, many cone-enriched genes show expression in additional retinal cell types (Fig. 2, SI Figs. 7 and 8, Table 1, and SI Table 6). For example, many cone genes show a cone + bipolar cell expression pattern (Fig. 2 *C*, *E*, *H*, and *I* and SI Table 6). Two cone genes show patterns of expression suggesting coexpression in cones and amacrine cells (*Cxx1c* and *A930018M24Rik*). Others show relatively diffuse staining throughout the inner nuclear layer and ganglion cell layer suggesting expression in multiple cell types (*Cltb*, *Enpp5*, and *Hist3h2ba*; Fig. 2*G*). Combined expression in cones and ganglion cells only has been reported in the chick (*Slc24a2*) but is so far unattested in the mouse (10). Lastly, many cone-enriched genes have additional expression domains outside of the retina (e.g., *Casp7*, *Adrb1*, *Ece1*, etc.). Although the range of biochemical functions assigned to these cone genes is broad, a number of the genes appear to be involved in metabolism of glucose/glycogen (*Pygm*, *Glo1*, and *Adrb1*), fatty acids (*Elovl2*), purine (*Ampd2*), and vitamin C (*Gulo*). Additionally, two genes involved in DNA repair (*Smug1*) and apoptosis (*Casp7*) were found to be cone-enriched. Corroborating one of these results, a recent paper showed that an antibody against glycogen phosphorylase (*Pygm*) specifically recognize cones in the mouse (11).

In silico mapping of photoreceptor-enriched transcripts to human chromosomal loci has contributed to the identification of retinal disease genes (1). We found that human orthologs of 9 of the 28 novel cone genes identified in our studies map in the region of uncloned human retinal disease loci (SI Table 6), making them promising disease gene candidates.

Dorsal–Ventral (D–V) Patterning of Photoreceptor Genes Suggests a Tripartite Classification of Expression Patterns. Detailed analysis of the expression pattern of the known and novel cone-enriched genes revealed three categories of D–V patterning: (*i*) pan-photoreceptor (with relatively uniform expression along the D–V axis); (*ii*) ventral > dorsal (similar to S-opsin); and (*iii*) dorsal > ventral (similar to M-opsin). The majority of cone genes showed a pan-photoreceptor pattern of expression and included previously known genes (e.g., *Gnat2*, *Gngt2*, and *Pde6c*) and novel cone genes (e.g., *Adrb1*, *E130012K09Rik*, and *7530404Mll-Rik*). Interestingly, one cone gene, *4921511K06Rik* showed an S-opsin-like pattern in which expression was largely absent in the dorsal third of the retina (Fig. 3). Strikingly, this gene is immediately adjacent to and divergently transcribed from the S-opsin locus in the mouse, suggesting that the similarities of their expression patterns may relate to transcriptional coregulation, possibly from a shared *cis*-regulatory element. Another new cone gene, *Smug1*, demonstrated an M-opsin-like pattern (dorsal > ventral). Although *Smug1*-positive cones were easily

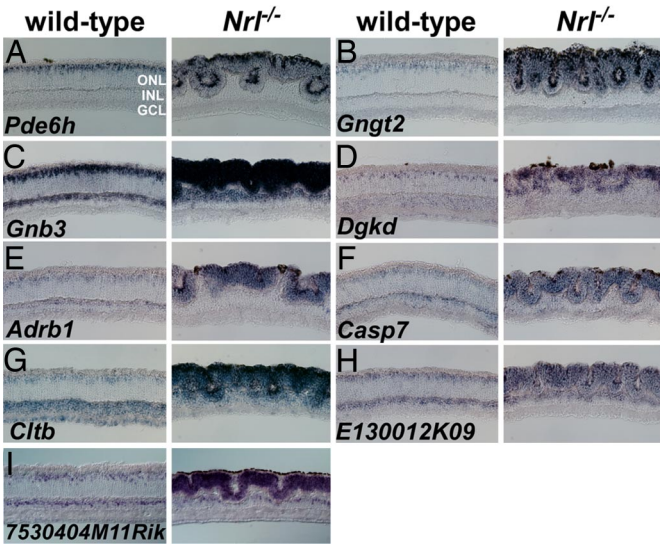

Fig. 2. Expression patterns of known and novel cone-enriched genes. (*A–C*) Expression patterns of known cone photoreceptor genes. *Pde6h* and *Gngt2* are expressed exclusively in cones, whereas *Gnb3* is strongly expressed in cones and bipolar cells. All three genes are markedly derepressed throughout the ONL in $Nrl^{-/-}$. (*D–I*) Expression pattern of some of the cone-enriched genes described in this study. *Dgkd* appears to be cone-specific. *Adrb1*, *E130012K09*, and *7530404M11Rik* are expressed in cones and bipolar cells. *Casp7* is expressed in cones and a subset of INL cells, possibly bipolar cells and/or horizontal cells. *Cltb* is expressed in cones and multiple inner retinal cell types. All of these genes show marked derepression throughout the ONL in $Nrl^{-/-}$. Expression patterns for all 73 genes in this study are presented in SI Figs. 3–8 and are summarized in SI Table 5. All sections are from young adult mouse retina.

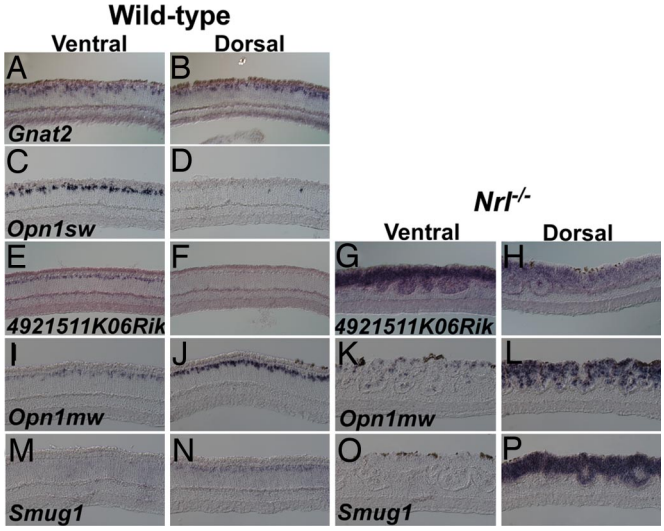

Fig. 3. D–V patterning of cone genes. (*A* and *B*) *Gnat2* is uniformly expressed along the D–V axis. (*C–F*) In contrast, *Opn1sw* (S-opsin) and *4921511K06Rik* show only rare positive cells in the dorsal third of the retina. (*I*, *J*, *M*, and *N*) *Opn1mw* (M-opsin) and *Smug1* are more strongly expressed in the dorsal retina than in the ventral portion. (*G*, *H*, *K*, *L*, *O*, and *P*) The D–V gradients of expression of *4921511K06Rik*, *Opn1mw*, and *Smug1* are accentuated in $Nrl^{-/-}$.

identified in the dorsal half of the WT retina (Fig. 3), they were not apparent in the ventral half. The similarity of this pattern to that of M-opsin was enhanced in the $Nrl^{-/-}$ retina, in which both M-opsin and *Smug1* showed marked derepression in the dorsal, but not the ventral retina (Fig. 3 *K*, *L*, *O*, and *P*). This pattern was opposite to that of *4921511K06Rik*, which shows an S-opsin-like pattern of expression (Fig. 3 *E–H*). Interestingly, the number of cells expressing *Smug1* in the $Nrl^{-/-}$ retina appeared to be greater than the number expressing *Opn1mw* (compare Fig. 3 *L* with *P*).

In our ISH screen of genes dysregulated in $Nrl^{-/-}$, we also identified a transcript with a rod-enriched pattern of expression which was asymmetrically expressed in a ventral > dorsal pattern. Further analysis confirmed that this transcript corresponds to a locus which is antisense to and immediately upstream of *Vax2* known as *Vax2os* (12) (SI Fig. 8). Interestingly, *Vax2os* is markedly down-regulated in both $Nrl^{-/-}$ and $Crx^{-/-}$ (SI Table 4 and ref. 38), whereas *Vax2* itself is unchanged in these backgrounds. To our knowledge, *Vax2os* represents the first rod-enriched gene known in the mouse to be asymmetrically expressed along the D–V axis.

To explore the possibility that additional photoreceptor genes might show an asymmetric pattern of expression along the D–V axis, we carried out an oligonucleotide microarray analysis of microdissected dorsal and ventral retina from P21 C57BL/6 mice (SI Table 8). Three biological replicates each of dorsal and ventral retina were examined, and up- and down-regulated genes were determined exactly as described for the $Nrl^{-/-}$ microarray experiments. We found that 67 genes were enriched in the ventral retina in two of three or three of three microarray comparisons (SI Table 9). Exactly the same number of genes was found to be enriched in the dorsal retina, using the same criteria (SI Table 10). Five of the 10 most highly enriched "dorsal" genes were genes previously shown to be enriched in the dorsal retina: *Tbx5*, *Ephrin B2* (*Efnb2*), COUP-TFII (*Nr2f2*), Raldh1 (*Aldh1a1*), and *Cyb1b1* (13–18). In addition, the two dorsal > ventral cone genes discussed above, *Opn1mw* (M-opsin), *Smug1*, and one additional cone gene, *Arr3*, were also found to be among the top 21 most dorsally enriched genes. Subsequent inspection of the ISH results for *Arr3* confirmed that there is a definite dorsal > ventral gradient of expression.

The first and third most enriched genes in the ventral retina were *Vax2OS* and *Vax2*, respectively. In addition, the two cone genes shown by ISH to be ventrally enriched, *Opn1sw* (S-opsin) and *4921511K06Rik*, were in the top 12 most enriched ventrally. Strikingly, four additional cone genes included in the present study, *Cxx1c*, *Kcne2*, *Ampd2*, and *Cabp5*, were within the top 63 genes most enriched in the ventral retina (SI Table 9). The presence of a ventral > dorsal expression gradient for these genes could not be assessed by ISH on account of the weakness of the signals. Cone-enriched genes therefore represent nearly 10% (6/63) of the most ventrally enriched genes in the mouse retina. These six cone genes represent ≈14% (6/44) of all cone genes in the present study, whereas the 67 most ventrally enriched genes represent only ≈0.26% (67/25,317) of all genes estimated to be present on this microarray. There is therefore a 52-fold enrichment of cone genes in the ventrally enriched group compared with what would be expected if cone genes were randomly distributed along the spectrum of D–V enrichment. Even the three dorsally enriched cone genes represent a 26-fold enrichment over a chance distribution. These findings suggest that cone genes with similar asymmetric distributions along the D–V axis may share common mechanisms of transcriptional regulation.

Discussion

In this study, we have defined a typology of rod and cone gene expression patterns in the mouse and have shown that accurate predictions of photoreceptor gene expression patterns can be derived from analysis of microarray data alone. Photoreceptor genes can range from entirely rod- or cone-specific to show varying degrees of rod/cone coexpression. In addition, they can be further classified according to their D–V pattern and their

pattern of expression in a variety of transcription factor mutant backgrounds. The present expression analysis complements two previous microarray studies by Yoshida *et al.* (7) and Yu *et al.* (19), wherein they carried out detailed functional classification and characterization of the genes dysregulated in $Nrl^{-/-}$. Using our "low stringency" cutoff, we found that our *Nrl*-up-regulated and down-regulated data sets included 76% and 82%, respectively, of the up- and down-regulated genes identified by Yoshida *et al.* (7) (data not shown; see SI Tables 3 and 4 for those "high stringency" genes shared between the two studies). In addition, a subset of the 18 cone-enriched genes identified in the present study (*Adrb1*, *Casp7*, *Clca3*, *Cltb*, *Olfm1*) were previously shown to be up-regulated in $Nrl^{-/-}$. However, in that study they did not perform ISH to prove that these genes were, in fact, cone-enriched.

Using identical cut-off thresholds, there are more than twice as many up-regulated genes than down-regulated in the $Nrl^{-/-}$ retina. One interpretation of this result is that a significant number of the up-regulated genes represent a response to injury in this retinopathic background. However, this is unlikely to account for the magnitude of the difference because there are only 691 up-regulated genes in the *Crx* mutant retina by the same criteria (38). Given that the *Crx* mutation results in a greater degree of retinal abnormality and more rapid photoreceptor cell death than the *Nrl* mutant (5, 20), one would expect, if anything, a greater up-regulation of injury-response genes in that background. Another interpretation is that in the mouse retina, there are a greater number of genes which show cone-enrichment than rod-enrichment.

Many rod and cone genes have additional retinal and extraretinal sites of expression. Among those photoreceptor genes with an additional site of expression within the retina, photoreceptor + bipolar cell expression is the single most common type. Studies have suggested a close cell fate relation between photoreceptors and bipolar cells (21, 22), and studies of the mouse S-opsin promoter region showed that short upstream regions drive reporter gene expression in both cones and bipolar cells (23, 24). Crx, a factor critical for transcription of many photoreceptor genes, is also expressed by bipolar cells. Furthermore, photoreceptors and bipolar cells elaborate an unusual structure, the ribbon synapse, which, within the retina, is unique to these two cells types. All of these similarities between photoreceptors and bipolar cells suggest common features in the *cis*-regulatory control of gene expression in these cells.

In the present study, we showed that a number of photoreceptor genes are expressed in D–V patterns similar to those of S- and M-opsin suggesting that they are under similar transcriptional control. It is known that in the *thyroid hormone receptor β2* (*TRβ2*) mutant mouse, M-opsin expression is lost and S-opsin is derepressed in the dorsal retina (25). Another study has demonstrated the appearance of a dorsal > ventral gradient of thyroid hormone in the mouse retina around the time of M-opsin expression onset (26), strongly implicating liganded TRβ2 in the formation of the M-opsin gradient. Interestingly, we found that type II deiodinase (*Dio2*), an enzyme required for converting an inactive form of thyroid hormone into its active form, T3, is among the top 20 most dorsally enriched genes in the mouse retina at P21 (SI Table 9). This asymmetric expression of *Dio2* may mediate the formation of the M-opsin gradient by the creation of a corresponding gradient of T3. In addition, we suggest that the asymmetric expression of a number of the other cone genes analyzed in the present study may be due to graded regulation by TRβ2.

A recent study demonstrated up-regulation of *endothelin 2* (*Edn2*) in photoreceptors in response to injury induced by several stimuli including bright light exposure, retinal detachment, and certain genetic retinopathies (27). Surprisingly, we found that *Edn2* is the third most dorsally enriched gene in the C57BL/6 retina at P21 (SI Table 9). Furthermore, *Edn2* is down-regulated almost 10-fold in the $Nrl^{-/-}$ retina suggesting that its expression is rod-specific (SI Table 4). These finding suggest the presence of a low-grade injury response in the dorsal retina of the WT C57BL/6 mouse. In further support of this idea, we also found that *ceruloplasmin* (*Cp*) and *glial fibrillary acidic protein* (*Gfap*), both expressed in Müller glia in response to injury (28, 29), are also dorsally enriched (SI Table 10). Lastly, one of the dorsally enriched cone genes we identified, *Smug1*, encodes a DNA repair enzyme (30). Another potentially related finding is that *complement factor I* (*Cfi*) was the fifth most dorsally enriched gene in the mouse (SI Table 10). *Cfi* acts in conjunction with *complement factor H* (*Cfh*) to modulate the alternative complement pathway (31). Because *Cfh* is the first gene found to confer a significantly increased risk of age-related macular degeneration in patients with unfavorable alleles (32–34), *Cfi* may also be involved in age-related macular degeneration pathogenesis, and its up-regulation may represent an early step in an injury response pathway in photoreceptors.

The reason for the increased expression of these injury response genes in a WT retina is currently not known but could possibly relate to differential exposure to light under animal facility conditions. Preferential photoreceptor cell death in the dorsal retina in response to bright light exposure is well-documented in both rats and zebrafish (35, 36). It is possible that this asymmetric susceptibility to injury is mediated by the differential expression of some of the genes analyzed in the present study.

Materials and Methods

Microarray Analysis of the *Nrl* Mutant. Microarray analysis of P21 $Nrl^{-/-}$ retinas was performed on Affymetrix mouse genome 430 2.0 GeneChip arrays (Affymetrix, Santa Clara, CA). A total of six microarray hybridizations were performed, three with probes derived from RNA from $Nrl^{-/-}$ (which is on a C57BL/6 background) and three from the corresponding WT strain, C57BL/6. For each microarray, RNA was prepared from four to six freshly dissected retinas derived from two to three animals at P21. Probes were synthesized starting with 10 μg of total RNA for each sample according to manufacturer's instructions (Affymetrix). Hybridization, washing, and scanning of the microarrays were all performed at the Bauer Center for Genomics Research at Harvard University according to manufacturer's instructions (Affymetrix).

Initial data analysis was carried out by using the GeneChip Operating System software from Affymetrix. Pairwise comparisons were made between individual mutant microarray results and controls. For our low stringency analysis, up- and down-regulated genes were determined by using Wilcoxon's signed rank test to compare mutant and control microarrays in a pairwise fashion with a P value of 0.002. Only those array features which were significantly "increased" or "decreased" in three of three microarray comparisons were considered to have met our criteria for inclusion in the low stringency data sets. To create a high stringency data set, we first separated the features in the low stringency data sets into three expression level categories: (for analysis of down-regulated features) (*i*) features whose average microarray score in the WT retina ($score_{B6}$) is ≥5,000; (*ii*) $1{,}000 \leq score_{B6} < 5{,}000$; and (*iii*) $100 \leq score_{B6} < 1{,}000$. For analysis of up-regulated features, the same categories were created by using the average microarray score for $Nrl^{-/-}$. Next, we sorted each of these three sublists according to the ratio of their average WT to average $Nrl^{-/-}$ scores and retained only those features that passed the following thresholds for the three expression categories: (*i*) at least a 2-fold change, (*ii*) at least a 3-fold change, and (*iii*) at least a 5-fold change. In this manner, we applied progressively more stringent fold-change requirements for the features showing lower levels of expression. Next,

to create a nonredundant list of up- and down-regulated genes (because our initial feature lists contained multiple features which correspond to a single gene) we used the DAVID functional annotation tool (http://david.abcc.ncifcrf.gov/) to annotate the following four lists: two low stringency (up- and down-regulated) and two high stringency (up- and down-regulated). We then wrote a Perl script to sort and format the DAVID outputs (script available on request).

Microarray Analysis of Dorsal and Ventral Retina. The dorsal and ventral thirds of the retina from 27 P21 mice (C57BL/6) were dissected by using iridectomy scissors, placed in an Eppendorf (Boulder, CO) tube, and frozen in dry ice. Approximately 18 pieces of dorsal and ventral retina were used to make each RNA prep (i.e., a total of three ventral and three dorsal preps). An average of 29 micrograms of total RNA was obtained from each preparation. Five micrograms were used for microarray probe synthesis. All subsequent microarray processing was as described above except that it was performed at the Genechip facility of the Siteman Cancer Center (Washington University, St. Louis, MO). Up- and down-regulated lists of genes were obtained by pairwise comparison of ventral and dorsal microarray results, using Wilcoxon's signed rank test with a cut-off P value of 0.002. To decrease the likelihood of missing asymmetrically expressed genes with only shallow D–V expression gradients, we chose to consider genes to be dorsally or ventrally enriched if they were shown to be enriched in two of three or three of three microarray comparisons.

RNA ISH. ISH on tissue sections was performed essentially as described in ref. 37. Retinas were dissected from 6- to 9-week-old $Nrl^{-/-}$ and WT (C57BL/6) mice in PBS and immediately put in 4% paraformaldehyde fixative at 4°C overnight. Tissue was equilibrated in 30% sucrose and then embedded in OCT compound. ISH with a given probe was generally performed on three or four retinas from two or three different mice (for each genotype). Sectioned tissue was hybridized with RNA riboprobes synthesized from PCR products derived from the templates indicated in SI Table 5.

We thank A. Swaroop (University of Michigan, Ann Arbor, MI) for the $Nrl^{-/-}$ mice, J. Trimarchi for discussions and early contributions to this work, and D. Kim for bringing the cone-enriched expression pattern of *Dgkd* to our attention. This work was supported the Foundation for Retina Research, the Howard Hughes Medical Institute, and National Institutes of Health Grants R01EY08676 (to C.L.C.) and K08EY014822 (to J.C.C.). C.L.C. is an Investigator of the Howard Hughes Medical Institute.

1. Blackshaw S, Fraioli RE, Furukawa T, Cepko CL (2001) *Cell* 107:579–589.
2. Hicks D, Sahel J (1999) *Invest Ophthalmol Vis Sci* 40:3071–3074.
3. Kefalov V, Fu Y, Marsh-Armstrong N, Yau KW (2003) *Nature* 425:526–531.
4. Ahnelt PK, Kolb H (2000) *Prog Retin Eye Res* 19:711–777.
5. Mears AJ, Kondo M, Swain PK, Takada Y, Bush RA, Saunders TL, Sieving PA, Swaroop A (2001) *Nat Genet* 29:447–452.
6. Daniele LL, Lillo C, Lyubarsky AL, Nikonov SS, Philp N, Mears AJ, Swaroop A, Williams DS, Pugh EN, Jr (2005) *Invest Ophthalmol Vis Sci* 46:2156–2167.
7. Yoshida S, Mears AJ, Friedman JS, Carter T, He S, Oh E, Jing Y, Farjo R, Fleury G, Barlow C, *et al.* (2004) *Hum Mol Genet* 13:1487–1503.
8. Corbo JC, Cepko CL (2005) *PLoS Genet* 1:e11.
9. Jadhav AP, Mason HA, Cepko CL (2006) *Development (Cambridge, UK)* 133:913–923.
10. Prinsen CF, Szerencsei RT, Schnetkamp PP (2000) *J Neurosci* 20:1424–1434.
11. Haverkamp S, Wassle H, Duebel J, Kuner T, Augustine GJ, Feng G, Euler T (2005) *J Neurosci* 25:5438–5445.
12. Alfano G, Vitiello C, Caccioppoli C, Caramico T, Carola A, Szego MJ, McInnes RR, Auricchio A, Banfi S (2005) *Hum Mol Genet* 14:913–923.
13. Koshiba-Takeuchi K, Takeuchi JK, Matsumoto K, Momose T, Uno K, Hoepker V, Ogura K, Takahashi N, Nakamura H, Yasuda K, Ogura T (2000) *Science* 287:134–137.
14. Braisted JE, McLaughlin T, Wang HU, Friedman GC, Anderson DJ, O'Leary DD (1997) *Dev Biol* 191:14–28.
15. McCaffery P, Wagner E, O'Neil J, Petkovich M, Dräger UC (1999) *Mech Dev* 85:203–214.
16. McCaffery P, Lee MO, Wagner MA, Sladek NE, Dräger UC (1992) *Development (Cambridge, UK)* 115:371–382.
17. Stoilov I, Rezaie T, Jansson I, Schenkman JB, Sarfarazi M (2004) *Mol Vis* 10:629–636.
18. Sen J, Harpavat S, Peters MA, Cepko CL (2005) *Development (Cambridge, UK)* 132:5147–5159.
19. Yu J, He S, Friedman JS, Akimoto M, Ghosh D, Mears AJ, Hicks D, Swaroop A (2004) *J Biol Chem* 279:42211–42220.
20. Furukawa T, Morrow EM, Li T, Davis FC, Cepko CL (1999) *Nat Genet* 23:466–470.
21. Ezzeddine ZD, Yang X, DeChiara T, Yancopoulos G, Cepko CL (1997) *Development (Cambridge, UK)* 124:1055–1067.
22. Altshuler D, Cepko C (1992) *Development (Cambridge, UK)* 114:947–957.
23. Chiu MI, Nathans J (1994) *J Neurosci* 14:3426–3436.
24. Chen J, Tucker CL, Woodford B, Szel A, Lem J, Gianella-Borradori A, Simon MI, Bogenmann E (1994) *Proc Natl Acad Sci USA* 91:2611–2615.
25. Ng L, Hurley JB, Dierks B, Srinivas M, Salto C, Vennstrom B, Reh TA, Forrest D (2001) *Nat Genet* 27:94–98.
26. Roberts MR, Srinivas M, Forrest D, Morreale de Escobar G, Reh TA (2006) *Proc Natl Acad Sci USA* 103:6218–6223.
27. Rattner A, Nathans J (2005) *J Neurosci* 25:4540–4549.
28. Chen L, Dentchev T, Wong R, Hahn P, Wen R, Bennett J, Dunaief JL (2003) *Mol Vis* 9:151–158.
29. Lewis GP, Fisher SK (2003) *Int Rev Cytol* 230:263–290.
30. Fromme JC, Banerjee A, Verdine GL (2004) *Curr Opin Struct Biol* 14:43–49.
31. Soames CJ, Sim RB (1997) *Biochem J* 326 (Pt 2):553–561.
32. Haines JL, Hauser MA, Schmidt S, Scott WK, Olson LM, Gallins P, Spencer KL, Kwan SY, Noureddine M, Gilbert JR, *et al.* (2005) *Science* 308:419–421.
33. Edwards AO, Ritter R, 3rd, Abel KJ, Manning A, Panhuysen C, Farrer LA (2005) *Science* 308:421–424.
34. Klein RJ, Zeiss C, Chew EY, Tsai JY, Sackler RS, Haynes C, Henning AK, SanGiovanni JP, Mane SM, Mayne ST, *et al.* (2005) *Science* 308:385–389.
35. Gordon WC, Casey DM, Lukiw WJ, Bazan NG (2002) *Invest Ophthalmol Vis Sci* 43:3511–3521.
36. Vihtelic TS, Soverly JE, Kassen SC, Hyde DR (2006) *Exp Eye Res* 82:558–575.
37. Chen CM, Cepko CL (2000) *Mech Dev* 90:293–297.
38. Hsiau TH-C, Diaconu C, Myers CA, Lee J, Cepko CL, Corbo JC (2007) *PLoS One*, in press.